Hindawi
International Journal of Geophysics
Volume 2022, Article ID 4883155, 11 pages
https://doi.org/10.1155/2022/4883155

Research Article

Recurrent Events' Impacts on foF2 Diurnal Variations at Dakar Station during Solar Cycles 21-22

Sibri Alphonse Sandwidi and Frédéric Ouattara

Laboratoire de Recherche en Energétique et Météorologie de l'Espace (LAREME), Université Norbert Zongo (UNZ), Koudougou, Burkina Faso

Correspondence should be addressed to Sibri Alphonse Sandwidi; alphonse.sandwidi@yahoo.fr

Received 28 July 2021; Revised 23 April 2022; Accepted 20 May 2022; Published 7 June 2022

Academic Editor: Angelo De Santis

This paper deals with recurrent events' (REs') impacts on foF2's diurnal variations at Dakar station (lat: 14.8° N, long: 342.6° E, Senegal) during solar cycles 21 and 22. Data were analyzed by taking in account solar phases and seasons influence. REs generate positive storms in all seasons and on all solar phases and also weak negative storms in all seasons and at minimum and maximum solar phases. The results suggest on the one hand that vertical drift $E \times B$ due to strong electrojet currents cannot be considered an important mechanism of positive storms and on the other hand that prereversal enhancement (PRE) phenomenon (with a delay due to Dakar station position) and equatorward thermospheric neutral winds circulation (TNWC) contribute mainly to their generation. The intense positive storms, which appear mostly at night, are observed in decreasing phase and in spring which correspond, respectively, to the solar phase and the season of maximum REs occurrence. Then, positive storms' strength presents seasonal and solar cycle dependence and it is related to REs days occurrence. REs' negative storms strength are linked directly with REs days' occurrence on solar phase scale, while they are not on seasonal scale.

1. Introduction

Ionospheric storms are disturbances during intense solar activities that cause abnormal variations in ionosphere's electron density [1–5]. These storms are associated by an increase or a decrease in electron density of ionospheric layers depending on whether the storm is positive or negative [2, 6–10]. While intense negative storms can cause serious problems (e.g., block out) in HF radiocommunication, severe positive storms cause problems such as scintillations, ionospheric delays, and errors in satellite communication and navigation [8, 9, 11].

At low and middle latitudes, three main mechanisms have been mentioned to explain the positive storms: (i) the equatorial electrojet (EEJ) [12–17], (ii) the prereversal enhancement (PRE) phenomenon [18, 19], and (iii) the equatorward thermospheric neutral wind circulation (TNWC) [12, 17, 20–23]. The PRE is a sharp eastward intensification of the daytime electric field near the magnetic equator shortly after sunset and before its reversal to westward [18]. The EEJ is an intense eastward current flowing near the magnetic equator. It is responsible of the equatorial ionization anomaly (EIA) region which is characterized by the diurnal formation of (i) the ionization trough near the magnetic equator and (ii) two ionization maxima located $\sim \pm 15°$ from the magnetic equator [24–27].

Concerning negative storms, Prölss [9] and Fuller-Rowell et al. [2] suggest that they arise from the thermospheric composition changes during magnetic storms which cause the augmentation in nitrogen's (N_2) and the drop in oxygen (O) one, so as to accelerate the recombination process (responsible of ionospheric electron density drop) during the storm. There are two types of recombination: (i) dissociative recombination ($AB^+ + e^- \longrightarrow A + B$) and (ii) radiative recombination ($A^+ + e^- \rightarrow A + h\vartheta$) [28]. The charge exchange processes such as $O^+ + N_2 \rightarrow NO^+ + N$ and $N^+ + O_2 \rightarrow NO^+ + O$ are the first step of the dissociative recombination ($NO^+ + e^- \rightarrow N + O$). Therefore, this recombination speed depends in the N_2/O ratio, whose peaks can so be considered a main reason of negative storms.

Statistical studies were carried out on foF2 variations by geomagnetic activity class as defined by Legrand and Simon's [29] classification which is defined as the ancient classification (AC) in this paper. The equivalence of the recurrent activities' (RAs) class in the AC is recurrent events' (REs') class in the new classification (NC) [30]. One of the novelties in this article is that this is the first time such study has been done considering the NC. Studies by Zerbo et al. [31] and Sawadogo et al. [32] have shown that RAs are predominant in decreasing solar phase and in spring. Sawadogo et al. [32] and Guibula [33], by studying RAs' impact on foF2 variations, respectively, at Ouagadougou (lat: 12.4° N, long: 358.5° E, Burkina Faso) and Korhogo (lat. 9.3° N; long. 354.62 E, Cote d'Ivoire) stations, found that RAs cause (i) positive storms during all solar phases and over seasons with maximum intensity by night, (ii) some sporadic negative storms, and (iii) EEJ current inhibition during seasons and also over solar phases. This study is aimed at analyzing REs' effects on foF2 variations during solar cycles 21 (SC 21) and 22 (SC 22) at Dakar station (lat: 14.8°N, long: 342.6° E, Sénégal) which is at about 8.1° N from the magnetic equator [34, 35].

Section 2 concerns the materials and methods. The results and discussions are presented in Section 3. Conclusion and perspectives are presented in Section 4.

2. Materials and Methods

This paper is aimed at comparing the foF2 diurnal variation during REs to those of very quiet activities (VQAs). Solar phases and seasons influence is taking account. Such diurnal profiles are analyzed in relation to the five standard profiles of Faynot and Vila [36].

2.1. Solar Phase Determination Criteria. Solar phases of SC 21 and SC 22 are determined by using the classification criteria related to the annual average of sunspot number Rz. These criteria, validated by Ouattara and Amory-Mazaudier [37], Ouattara et al. [38], Zerbo et al. [39], and Gnabahou and Ouattara [40] are defined as follows: (i) minimum phase: $Rz < 20$; (ii) increasing phase: $20 \leq Rz \leq 100$ with Rz greater than that of the previous year; (iii) maximum phase: $Rz > 100$ noting that for weak solar cycles (with $Rz_{max} < 100$) maximum phase's years correspond to those with an index $Rz > 0,8.Rz_{max}$, and (iv) decreasing phase: $100 \geq Rz \geq 20$ with Rz lower than that of the previous year.

2.2. Season Determination Criteria. Several studies have proven the seasonal dependence of foF2 variations in relation to geomagnetic activity. Some of these studies have highlighted the existence of semiannual variation, characterized by peaks in diurnal foF2 values at equinoxes [41, 42] while others reveal the existence of winter anomaly characterized by peaks of foF2 in winter compared to summer [43–45]. The seasons are defined as follows: (1) spring (March, April, and May); (2) summer (June, July, and August); (3) autumn (September, October, and November), and (4) winter (December, January, and February).

2.3. Methods for Determining Geomagnetic Activity. Legrand and Simon [29] and Richardson et al. [46–48] classified geomagnetic activity into four classes based on criteria taking into account solar activity, sudden storm commencement (SSC) dates, and aa index values. An SSC corresponds to an abrupt change in the geomagnetic field followed by a geomagnetic storm that lasts less than an hour [49, 50]. The SSC index is identified by the date and time the storm occurred. The geomagnetic index aa is deduced from the K index measured at two antipodal stations in the middle latitude. The K index is an integer between 0 and 9 corresponding to a class that contains the largest range of geomagnetic disturbances in the two horizontal components [51]. The arithmetic means of the eight index values aa measured each day in accordance with the eight daily trihourly index values K is denoted Aa. Dates of SSCs and aa index values are available from 1869 to present on the ISGI website (http://isgi.unistra.fr).

Recently, Zerbo et al. [30] proposed a new classification (NC) which pushes back the limits of the AC by providing clarifications on the solar origin of about 20% of geomagnetic storms in addition to the 60% explained by the AC. In the NC, quiet activity days, associated with slow solar winds, correspond to days when $Aa < 20$ nT and disturbed activity to days when $Aa \geq 20$ nT. The latter include (i) fluctuating activity days (FAs) or fluctuating events (FEs) caused by fluctuations in the sun's neutral blade, (ii) shock events (SEs) including shock activity (SA) of the AC (due to coronal mass ejections (CMEs)) and cloud shock activity (CSA) (due to magnetic clouds), and (iii) recurrent events days (REs). As in AC, the selection according to NC is done by using pixel diagram proposed by Legrand and Simon [29] and improved by Ouattara and Amory-Mazaudier [37] who organized it in columns and rows; then, they defined a color code to identify different types of geomagnetic activities.

Pixel diagram (Figure 1) represents the evolution of the geomagnetic index aa as a function of solar activity for each rotation of the sun or Bartels' rotation [52]. A line in the diagram represents a rotation of the sun (27 days). The SSC dates are indicated by circles surrounding the corresponding aa index value. The dates of the beginning days of the Bartels cycle, the legend and the year are indicated, respectively, on the left, on the right, and on the top of the diagram. In a pixel diagram, the REs are represented by

(i) classical recurrent activities of AC (RAs) due to fast solar winds which are a set of at least two successive days represented by orange, red, and/or dark red boxes on at least two days without SSC recurrence and on at least two solar rotations

(ii) corotating moderate activity days (CMAs), which are due to stable corotating solar winds and are represented by yellow and green boxes on at least two days without SSC recurrence and on at least two solar rotations

To better appreciate REs' impact, the VQAs considered correspond to the reference limits used by Zerbo et al. [39] and Gnabahou and Ouattara [40]. Note that for a given period, the VQAs' days ($Aa < 10$ nT) [53] boxes are white colored.

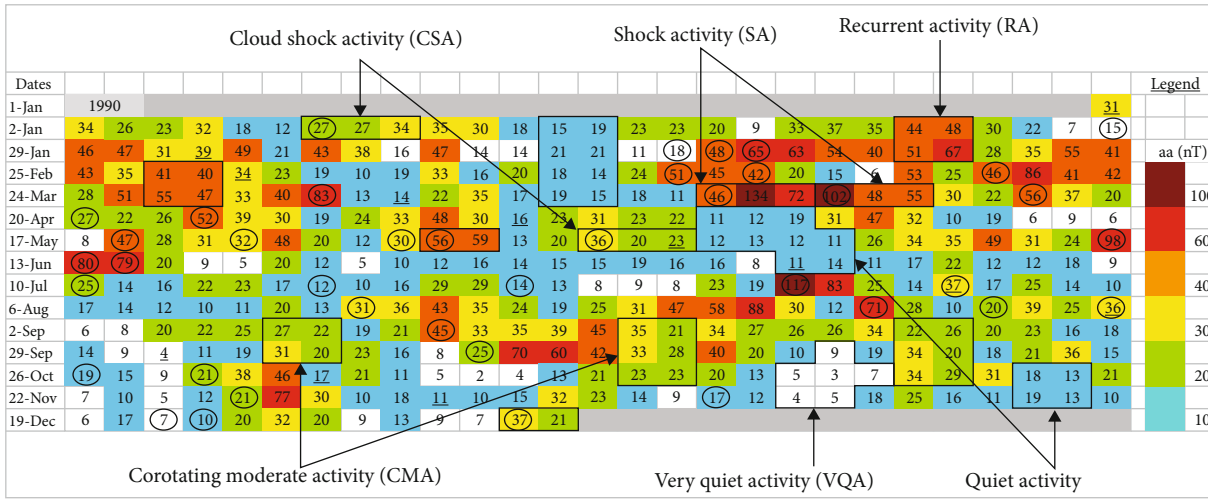

Figure 1: Pixel diagram showing different geomagnetic activities' classes according to NC [30].

2.4. Data Analysis Methods. The error bars placed on foF2 profiles of the VQAs, for the qualitative analysis of REs compared to VQAs, are obtained by $\delta = \sqrt{V}$ where V is the variance given by

$$V = \frac{\sum_{i=1}^{N} \left(\text{foF2}_i - \overline{\text{foF2}} \right)^2}{N}, \quad (1)$$

where foF2_i are the hourly foF2 values, $\overline{\text{foF2}}$ is hourly average of foF2_i values, and N the total number of days depending on the solar phase or season considered.

Then, based on the definition of storm strength as defined by Vijaya Lekshmi et al. [54], the relative deviation of foF2 (δfoF2), allowing the type and intensity of the observed storm to be assessed, is defined by

$$\delta\text{foF2} = \frac{\overline{\text{foF2}_d} - \overline{\text{foF2}_q}}{\overline{\text{foF2}_q}} \times 100, \quad (2)$$

where $\overline{\text{foF2}_d}$ and $\overline{\text{foF2}_q}$ denote the average hourly values of foF2, respectively, in disturbed periods and in very calm periods.

The storm is qualified as positive and negative, when δ foF2 > 0 and δfoF2 < 0, respectively.

For values of δfoF2 between $\mp$20%, the storm is considered moderate; otherwise, we are talking about an intense storm.

Likewise, based on the definition of Vijaya Lekshmi et al. [54], the storm's strength is analyzed between seasons or solar phases by the diurnal mean deviation of the storm. $\overline{\text{foF2}_{d,\text{diurnal mean}}}$ is diurnal mean of foF2 hourly values during disturbed days and $\overline{\text{foF2}_{q,\text{diurnal mean}}}$, that of calm days. Storms' strength is estimated by class (positive and negative) to better appreciate their strength and avoid balancing effects between positive and negative storms.

For positive storms, the diurnal means computed on hourly values are such that $\overline{\text{foF2}_d} > \overline{\text{foF2}_q}$. Thus, positive storm's strenght ($\Delta\text{foF2}^p_{\text{storm}}$) is defined by

$$\Delta\text{foF2}^p_{\text{storm}} = \overline{\text{foF2}_{d,\text{diurnal mean}}} - \overline{\text{foF2}_{q,\text{diurnal mean}}}. \quad (3)$$

For negative storms, the diurnal means computed on hourly values are such that $\overline{\text{foF2}_d} < \overline{\text{foF2}_q}$. Thus, negative storm's strenght ($\Delta\text{foF2}^n_{\text{storm}}$) is defined by

$$\Delta\text{foF2}^n_{\text{storm}} = \overline{\text{foF2}_{q,\text{diurnal mean}}} - \overline{\text{foF2}_{d,\text{diurnal mean}}}. \quad (4)$$

To analyze the occurrences of REs and VQAs days, recurrent and very quiet days during SC 21 and SC 22 (from 1 January 1976 to 31 December 1995) were counted. The study covered 1118 very quiet days and 648 recurrent days. Rates of occurrence are obtained using

$$\%\text{Occ} = \frac{N_A}{N_T} \times 100, \quad (5)$$

where N_A is the number of VQAs days or REs days over solar phase or the considered season and N_T the total number of days per solar phase or by the considered season.

3. Results and Discussion

3.1. Recurrent Activities' Occurrence per Season and per Solar Phase. Figure 2 gives the occurrence of REs and VQAs by solar phase ("a") and by season ("b"). VQAs are predominant than REs during all solar phases except at decreasing phase. Occurrence rates increase with solar cycle progression. Thus, both VQAs and REs appear less at solar minimum while they are predominant in the decreasing phase when a REs rate of 53.55% and a VQAs rate of 32.74% are obtained. VQAs predominate over REs during solstice months while REs preponderate during equinox months with rates of 32.7% in spring and 28.7% in autumn. This

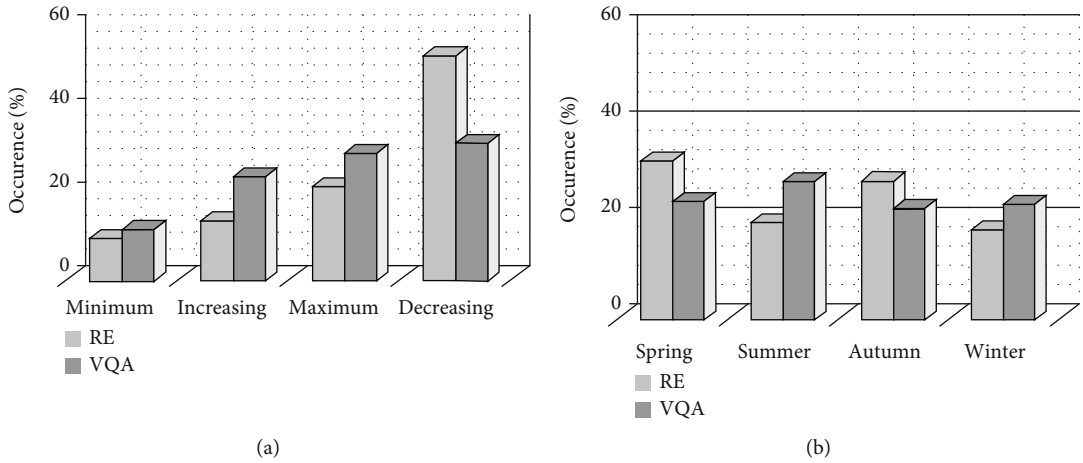

Figure 2: Recurrent events occurrence variability per solar phase (a) and per season (b).

highlights the presence of equinoctial and semiannual asymmetries in the seasonal occurrence of REs as shown by Sawadogo et al. [32] at Ouagadougou station.

3.2. Recurrent Events' (REs) Storm Effects per Solar Phase. Figure 3 shows foF2 diurnal variations profiles and the relative deviation δfoF2 between REs and VQAs. Solid curves and dashed curves relate, respectively, to VQAs and REs. These graphs are used to study REs' impact on foF2 variations by solar phase at Dakar station. Panels (a)–(d) are assigned, respectively, to minimum, increasing, maximum, and decreasing phases.

In panel (a), foF2's profiles show that REs do not disturb the "B"-shaped profile observed during VQAs. The evening peak of VQAs' curve is also observed during REs. VQAs' graph shows an increasing trend after midnight followed by a peak around 0100 LT. The one of REs shows an increasing trend from 2300 LT to midnight, followed by a decreasing trend from midnight to 0100 LT, when it started raising again up to a peak around 0200 LT. Thus, REs split the abnormality observed in recombination mechanism during VQAs from midnight to a double abnormality between 2300 LT and midnight, and from 0100 LT to 0200 LT, with an expected behavior of the recombination in between. δ foF2's graph indicates that at solar minimum REs cause positive storms during day time, except around 0600 LT where they produce a low negative storm because $\delta\text{foF2} < 0$. The strongest (intense) storms, characterized by $\delta\text{foF2} > 20\%$, occur at night with a peak observed at 0000 LT ($\delta\text{foF2} \sim 40\%$) and they are moderate during day time ($\delta\text{foF2} < 20\%$).

At panel (b), REs reproduce the ionization dip of 1200 LT. The evening peak observed on VQAs' curve is not modified by REs. foF2's graph indicates that REs cause positive storms during both daytime and nighttime. These storms are intense throughout the night (2100 to 0000 LT, around 0300 LT and 0500 LT) with a peak observed around 0000 LT ($\delta\text{foF2} \sim 34.3\%$). Storms are moderate the remaining time of the day.

At panel (c), REs' and VQAs' curves show a "P" profile. But the one of VQAs is associated with a slight morning peak and a barely noticeable ionization dip around local noon. An abnormal night peak is observed around 0100 LT during VQAs while it is observed one hour before (0000 LT) during REs, with a minor peak at 2200 LT. Although the minor peak at 2200 TL does not coincide with the PRE phenomenon (expected shortly after sunset (1700-1900 TL)), this observation can be linked to an expansion of the PRE with a delay due to Dakar station position. δ foF2's graph indicates that REs cause moderate storms during all daily time. Storms are usually positive with some low negative storms observed in morning (0700-0800 LT), around 2300 LT and 0100 LT.

In panel (d), the curves present a profile "B" with predominance of evening peak during VQAs and an "R" profile during REs. The local ionization dip around noon is typical on the equatorial zones and is related to EEJ current presence. Thus, its absence during the REs suggests that REs are favorable to EEJ current inhibition at decreasing phase. δfoF2's values indicate that observed storms are positive at all times, being intense by night ($\delta\text{foF2} > 20\%$ from 2200 to 0800 LT) and moderate during day.

3.3. Recurrent Events' (REs) Storm Effects per Season. Figure 4 shows foF2 diurnal variations profiles and relative deviation δfoF2 between REs and VQAs. Solid and dashed curves relate, respectively, to VQAs and REs. These graphs are used to study REs' impact on foF2 seasonal variations. Panels (a)–(d) are assigned, respectively, to spring, summer, autumn, and winter seasons.

At panels (a) and (b), curves show "R" profiles, showing therefore that REs do not modify the evening ionization peak observed during VQAs in spring and summer. Error bars show that, in spring, ionization during REs is greater during nighttime (2000-0500 LT). But in summer, REs' curve superimposes that of VQAs almost all the time. δfoF2's graph indicates that in spring REs cause moderate positive storms at daytime with a weak negative storm around 0800 LT and intense positive storms at night ($\delta\text{foF2} > 20\%$ from 2000 to 0500 LT, with a maximum δ foF2 greater than 80% around 0000 LT). On the other hand, in summer, we observe a moderate storm almost

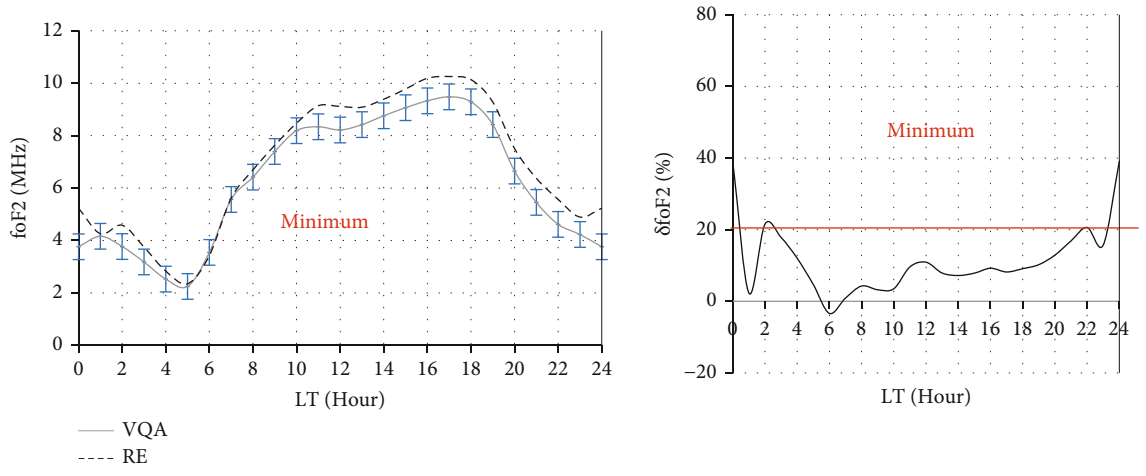

(a)

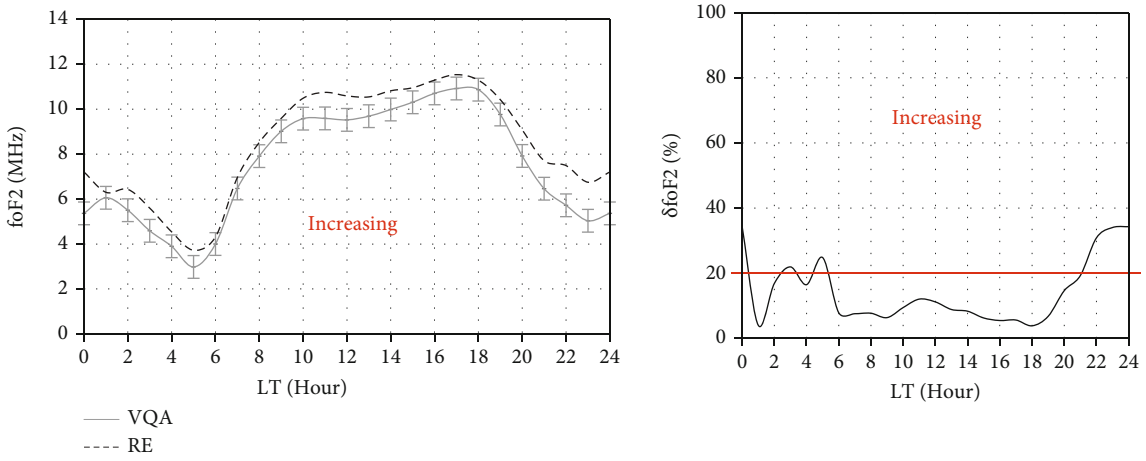

(b)

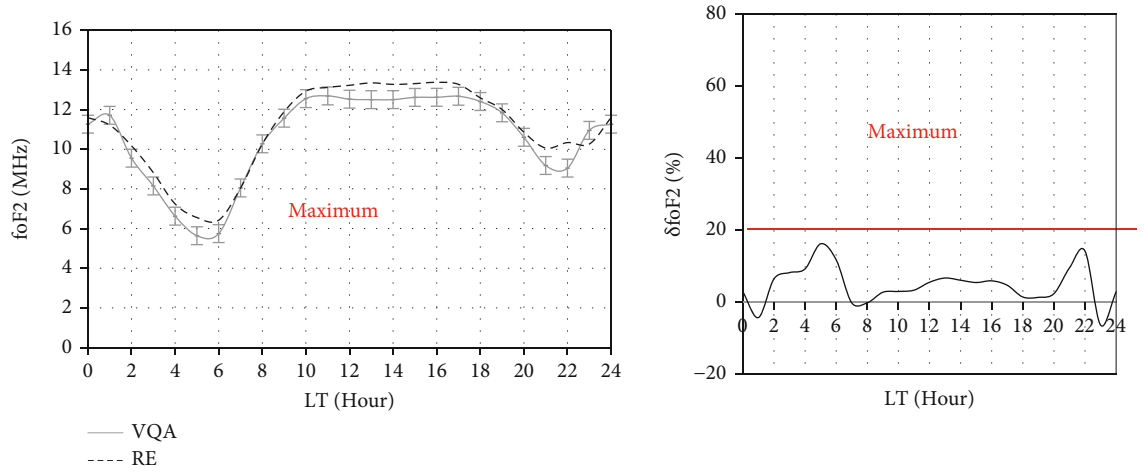

(c)

Figure 3: Continued.

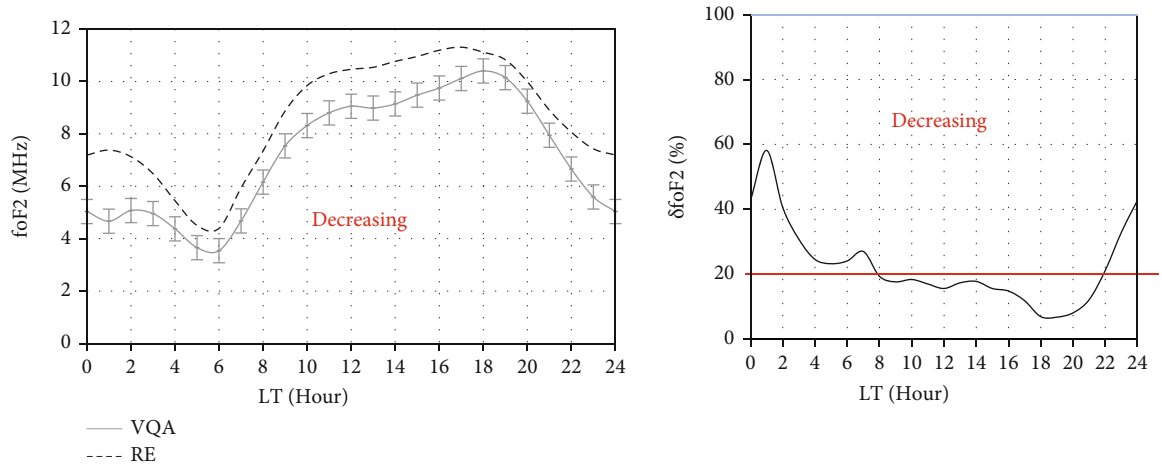

(d)

Figure 3: Solar phases' influence on foF2 diurnal variations during recurrent events (REs).

all the time with an oscillation of δfoF2 value sign, translating a fluctuation between negative storms (~0600 LT, 0800-1000 LT, and 1900-2300 LT) and positive storms during the remaining day time, with a maximum δfoF2 of 16.28% at ~0100 LT.

Panel (c) shows an ionization trough around local noon in autumn. δfoF2's graph indicates that in the autumn REs cause positive storms during daytime, except around 0100 LT and 0300 LT where negative storms appear. Storms are moderate at all times except around 0600 LT (δfoF2 ~ 22.22%). The REs' abnormal nocturnal peak is observed at 0000 LT though the one of VQAs is observed at 0100 LT.

At panel (d), curves show an "M" type profile, with a weak morning peak ionization and a little dip ionization around noon on VQAs' curve. Error bars show that in winter, ionization is greater at all times during REs compared to VQAs, except in morning (0700-1000 LT). The minor peak at 2200 LT on REs' curve can be linked to an expansion of the PRE with a delay due to Dakar station position. δfoF2's curve indicates that in winter REs cause negative storms in the morning (0700-0800 LT) and positive storms all the remaining time. Storms are moderate most of the time except around 0600 LT and from 2200 to 0000 LT.

3.4. Recurrent Events' Storm Strength on foF2 Variation by Solar Phase and by Season. Table 1 shows recurrent events positive storms' strength on foF2 variations over solar cycle and seasons. It is observed that the strongest storms appear during decreasing phase and spring months while the weakest are observed at solar maximum and in summer months.

Table 2 shows recurrent events' negative storms' strength on foF2 variations over solar cycle and seasons. Negative storms are not observed during increasing and decreasing solar phases. The strongest storms appear during maximum phase and autumn months while the weakest are observed at solar minimum and in spring months.

3.5. Discussions. From the analysis of REs impact on foF2 diurnal variations, it emerges that

(1) REs generate positive storms during all the daytime. Sawadogo et al. [32] found the same result by analyzing RAs' impact on foF2 diurnal variations at Ouagadougou station. Weak negative storms are observed at solar minimum (~0600 LT) and solar maximum (from 0700 to 0800 LT, ~2300 LT, and~0100 LT), in summer (~0500 LT, ~0900 LT and from 1900 to 2300 LT), in autumn (~ 0100 and~ 0300 LT), in winter (0700-0800 LT), and in spring (~ 0800 LT).

(2) Troughs are observed at noon local time in minimum, increasing and decreasing solar phases and autumn months. It is well known that with plasma fountain effects the tendency should be an increase in electron density at the tropics (~ ∓15° on either side of the magnetic equator) and an ionization dip at the magnetic equator around local noon [55]. Since Dakar station (lat: 14.8° N; long: 342.6° E) is at about 8.1° N from the magnetic equator which is at about 6.5° N at African sector [34, 35], it lies in the transition zone between EIA region trough and its crest. This explains the observation of the local noon trough under some solar activity and seasonal conditions, which favor an equatorial behavior rather than the one expected at the crests of the EIA region

(3) Storms' effect on vertical drift $E \times B$ disturbs foF2's diurnal profiles morphologies during disturbed activities [56]. This phenomenon is due to the midday EEJ current inhibition. It is observed during REs, especially over decreasing solar phase and in autumn months. Guibula's [33] works show that at Korhogo station (located in the hollow of the EIA region), this EEJ current inhibition at noon is observed in winter while those of Sawadogo et al.'s [32] which showed that at Ouagadougou station it

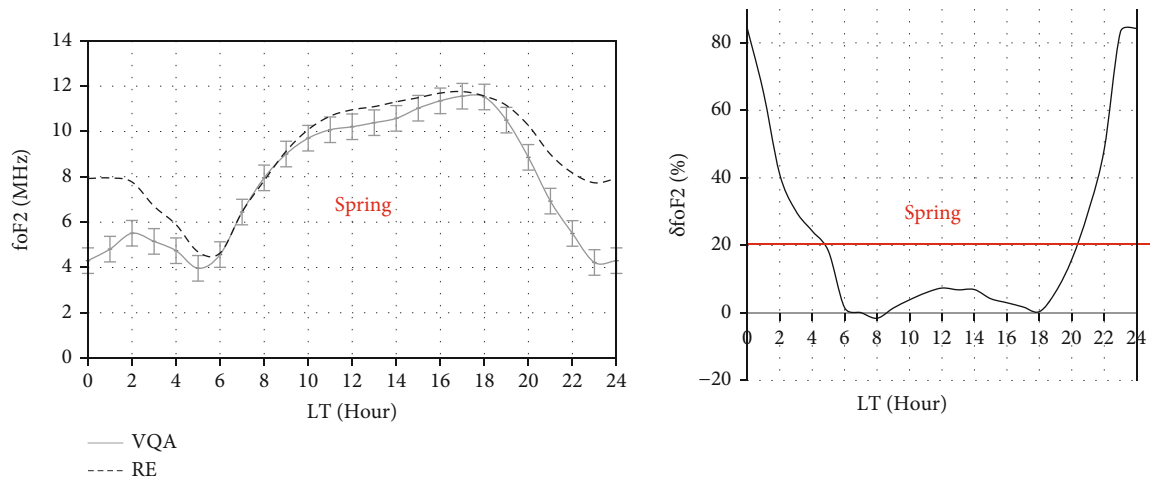

(a)

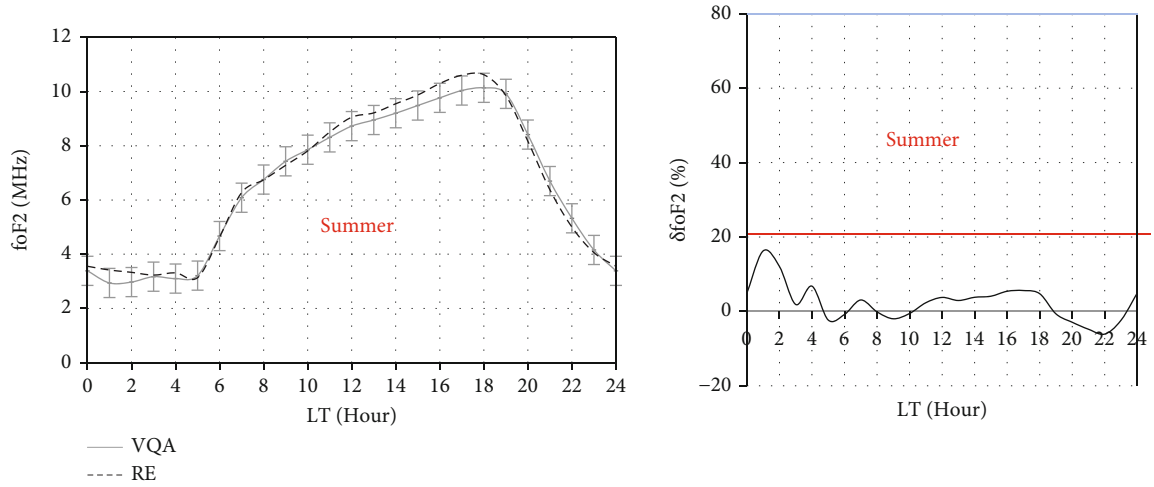

(b)

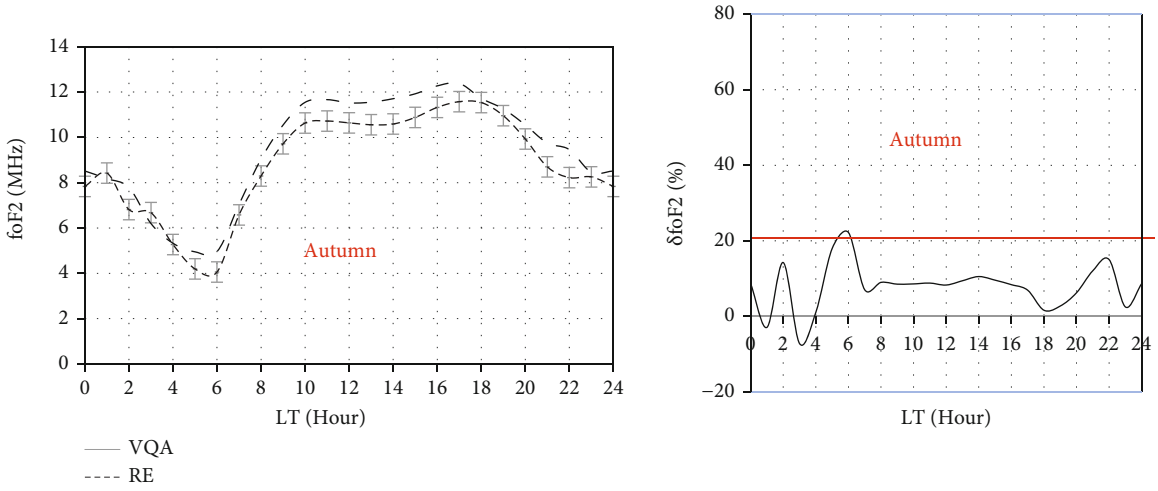

(c)

Figure 4: Continued.

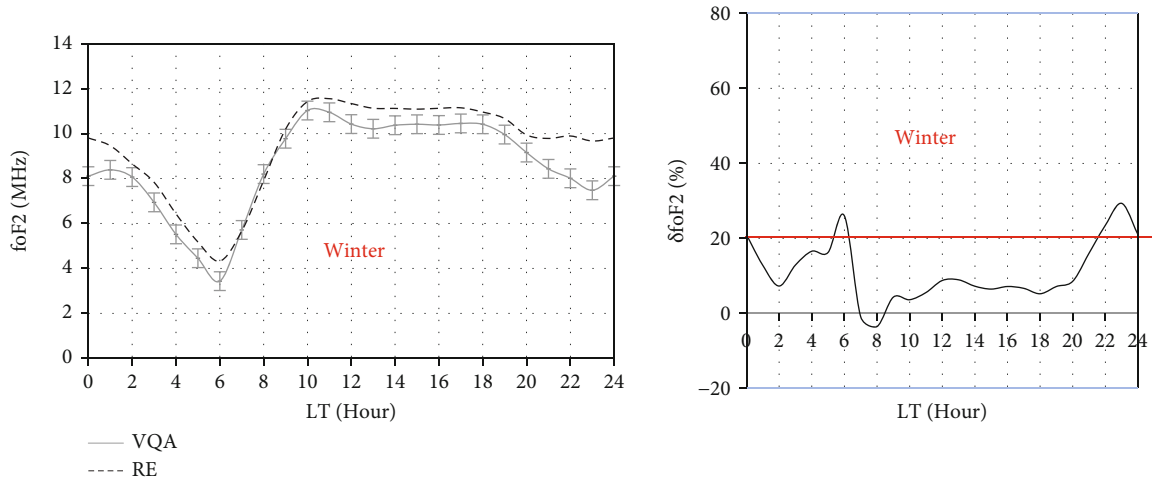

(d)

Figure 4: Seasons' influence on foF2 diurnal variations during recurrent events (REs).

Table 1: Recurrent events' positive storms strength on foF2 variation by solar phase and by season.

Storm strength over solar phases	Minimum	Increasing	Maximum	Decreasing
$\Delta foF2^{p}_{storm}$ (MHz)	0.64	0.88	0.61	1.38
Storm strength over seasons	Spring	Summer	Autumn	Winter
$\Delta foF2^{p}_{storm}$ (MHz)	1.18	0.33	0.76	0.93

Table 2: Recurrent events' negative storms strength on foF2 variation by solar phase and by season.

Storm strength over solar phases	Minimum	Increasing	Maximum	Decreasing
$\Delta foF2^{n}_{storm}$ (MHz)	0.12	—	0.30	—
Storm strength over seasons	Spring	Summer	Autumn	Winter
$\Delta foF2^{n}_{storm}$ (MHz)	0.13	0.14	0.36	0.17

is observed on all solar phases and only in summer at seasons scale. These differences could be explained by phenomena that are still poorly understood. Gnabahou et al. [34] suggested the position of those African EIA region stations as an explanation

(4) Minor peaks are observed at 2200 LT during maximum phase and winter season. It is also noted that REs are more favorable to 2200 LT minor peak appearance. Indeed, VQAs' curve during winter season present a little inflection around 2200 LT without however marking a real peak while at the same period of the day that of REs present a minor peak. It could be inferred that Dakar station behaves like a crest station during winter months and also during maximum phase for the same reason

(5) The strongest positive storms appear during decreasing phase and spring months while the weakest ones are observed at solar maximum and in summer months. REs are predominant in decreasing phase and in spring as observed, respectively, by Zerbo et al. [31] and Sawadogo et al. [32]. This suggests that positive storms' strength due to REs is related to REs' days occurrence

(6) As concern negative storms, the more intense are observed during maximum solar phase and autumn season and the weakest during minimum solar phase and spring season. At solar phase scale, REs are predominant at maximum than during minimum; and over seasons scale, they are predominant during spring than during autumn. This suggests that at solar phases scale negative storms' strength due to REs are related to REs' days occurrence while they are not on seasons scale

It is well known according to Prölss [9, 10] and Fuller-Rowell et al. [2] that negative storms result from variations in thermosphere composition during magnetic storms. We can therefore observe a moderate acceleration of the recombination process (with an increasing of N_2/O ratio) at solar minimum (~0600 LT), at maximum phase (~0100 LT, ~0700 LT, and ~2300 LT), in summer (~0500 LT, ~0900

LT, and 1900-2300 LT), in autumn (~0100 and ~0300 LT), and in winter (0700-0800 LT) during REs. One would therefore expect to observe the peak of recombination mechanism around 0100 LT in autumn of solar maximum during REs.

It was observed that electrojet intensity increases with solar activity [57–59]. However, the greater positive storms and most of negative storms are observed by night or at morning (not at noon), and positive storms of solar minimum are more powerful than those of solar maximum. Therefore, we could deduce that $E \times B$ drift due to strong diurnal EEJ cannot be considered a prevailing mechanism for storms' generation.

The observed positive storms around 2200 TL do not coincide with the PRE phenomena in winter and during maximum phase. The PRE is a sharp eastward intensification of the daytime electric field near the magnetic equator shortly after sunset and before its reversal to westward [18]. According to Farley et al. [18] and Kelley [19], this inversion is due to the effect of the zonal wind which induces an accumulation of electric charges at day-night (1700-1900 LT) boundary. There is thus strong reason to consider, in agreement with Dakar station position, that the minor peak around 2200 LT can be link to the PRE (with a delay) as a major mechanism of the positive storms observed after dusk.

Most positive storms are observed at night (when chemical recombination is predominant), especially in decreasing solar phase and in spring, when REs are predominant. According to Balan et al. [20], positive ionospheric storms are more likely to occur when the plasma accumulation due to the mechanical effects of TNWC exceeds the losses due to chemical recombination. This suggests that the TNWC from high to low latitudes [60] can be considered a major source of positive storms.

4. Conclusions

REs are predominant in equinox months (particularly in spring) and during solar decreasing phase and appear less in solstice months (particularly in winter) and in solar minimum. Morphological analysis of foF2 profiles during REs and VQAs at Dakar station shows that REs disrupt F2 layer electrodynamics during maximum and decreasing solar phases and in autumn and winter on seasons' scale. Equatorward TNWC and the PRE phenomenon (caused by the disturbance of zonal winds by REs) contribute mainly to positive storms. The strongest positive storms are observed in the decreasing phase and in spring months. This suggests that positive storms' strength due to REs is related to REs' day occurrence. The more intense negative storms are observed at maximum and autumn season and the weakest during minimum solar phase and spring season. This suggests that at solar phases scale negative storms' strength due to REs are related to REs' days occurrence while they are not on seasons' scale. The local noon trough and the abnormal night time peak observation under some solar activity and seasonal conditions suggested that Dakar station behaves like an equatorial station during all solar phases and seasons, except during maximum solar phase and winter months.

Data Availability

The sunspot data used to support the findings of our study are available at http://www.sidc.be/silso/datafiles. The geomagnetic aa index data are available at http://isgi.unistra.fr/data_download.php.

Conflicts of Interest

The authors declare no conflicts of interest.

Acknowledgments

The authors thank Brest Telecom of Bretagne for providing Dakar ionosonde data. Many thanks to ISGI data center for providing their data center.

References

[1] M. Blanc and A. D. Richmond, "The ionospheric disturbance dynamo," *Journal of Geophysical Research*, vol. 85, no. A4, pp. 1669–1686, 1980.

[2] T. Fuller-Rowell, M. Codrescu, R. Moffett, and S. Quegan, "Response of the thermosphere and ionosphere to geomagnetic storms," *Journal of Geophysical Research, Space Physics*, vol. 99, no. A3, pp. 3893–3914, 1994.

[3] S. Matsushita, "A study of the morphology of ionospheric storms," *Journal of Geophysical Research*, vol. 64, no. 3, pp. 305–321, 1959.

[4] A. D. Richmond and S. Matshushita, "Thermospheric response to a magnetic substorm," *Journal of Geophysical Research*, vol. 80, no. 19, pp. 2839–2850, 1975.

[5] Y. Sahai, P. R. Fagundes, F. Becker-Guedes et al., "Longitudinal differences observed in the ionospheric F-region during the major geomagnetic storm of 31 March 2001," *Annales Geophysicae*, vol. 22, no. 9, pp. 3221–3229, 2004.

[6] M. J. Buonsanto, "Ionospheric storms—a review," *Space Science Reviews*, vol. 88, no. 3/4, pp. 563–601, 1999.

[7] M. Buonsanto and O. Witasse, "An updated climatology of thermospheric neutral winds and F region ion drifts above Millstone Hill," *Journal of Geophysical Research, Space Physics*, vol. 104, no. A11, pp. 24675–24687, 1999.

[8] M. Mendillo, "Storms in the ionosphere: patterns and processes for total electron content," *Reviews of Geophysics*, vol. 44, no. 4, 2006.

[9] G. W. Prölss, "Ionospheric F-region storms," *Handbook of atmospheric electrodynamics*, vol. 2, pp. 195–248, 1995.

[10] G. W. Prölss, *Physics of the earth's space environment*, Universitat Bonn Institut fiir Astrophysik und Extraterrestrische Forschung, 2003.

[11] N. Balan, Y. Otsuka, M. Nishioka, J. Liu, and G. Bailey, "Physical mechanisms of the ionospheric storms at equatorial and higher latitudes during the recovery phase of geomagnetic storms," *Journal of Geophysical Research, Space Physics*, vol. 118, no. 5, pp. 2660–2669, 2013.

[12] N. Balan, K. Shiokawa, Y. Otsuka, S. Watanabe, and G. Bailey, "Super plasma fountain and equatorial ionization anomaly during penetration electric field," *Journal of Geophysical Research: Space Physics*, vol. 114, no. A3, 2009.

[13] A. Danilov, "F2-region response to geomagnetic disturbances," *Journal of Atmospheric and Solar - Terrestrial Physics*, vol. 63, no. 5, pp. 441–449, 2001.

[14] A. Danilov, "Ionospheric F-region response to geomagnetic disturbances," *Advances in Space Research*, vol. 52, no. 3, pp. 343–366, 2013.

[15] T. Kikuchi and T. Araki, "Horizontal transmission of the polar electric field to the equator," *Journal of Atmospheric and Terrestrial Physics*, vol. 41, no. 9, pp. 927–936, 1979.

[16] T. Kikuchi, H. Lühr, K. Schlegel, H. Tachihara, M. Shinohara, and T. Kitamura, "Penetration of auroral electric fields to the equator during a substorm," *Journal of Geophysical Research, Space Physics*, vol. 105, no. A10, pp. 23251–23261, 2000.

[17] A. Mannucci, B. T. Tsurutani, B. A. Iijima et al., "Dayside global ionospheric response to the major interplanetary events of October 29-30, 2003 "Halloween Storms"," *Geophysical Research Letters*, vol. 32, no. 12, 2005.

[18] D. Farley, E. Bonelli, B. G. Fejer, and M. Larsen, "The prereversal enhancement of the zonal electric field in the equatorial ionosphere," *Journal of Geophysical Research, Space Physics*, vol. 91, no. A12, pp. 13723–13728, 1986.

[19] M. Kelley, *The Earth's Ionosphere*, Academic, San Diego, California, 1989.

[20] N. Balan, K. Shiokawa, Y. Otsuka et al., "A physical mechanism of positive ionospheric storms at low latitudes and mid-latitudes," *Journal of Geophysical Research, Space Physics*, vol. 115, no. A2, 2010.

[21] M. C. Kelley, M. N. Vlasov, J. C. Foster, and A. J. Coster, "A quantitative explanation for the phenomenon known as storm-enhanced density," *Geophysical research letters*, vol. 31, no. 19, 2004.

[22] T. Kikuchi, T. Araki, H. Maeda, and K. Maekawa, "Transmission of polar electric fields to the equator," *Nature*, vol. 273, no. 5664, pp. 650-651, 1978.

[23] G. Prölss and M. Jung, "Travelling atmospheric disturbances as a possible explanation for daytime positive storm effects of moderate duration at middle latitudes," *Journal of Atmospheric and Terrestrial Physics*, vol. 40, no. 12, pp. 1351–1354, 1978.

[24] W. Baker and D. F. Martyn, "Electric currents in the ionosphere-the conductivity," *Philosophical Transactions of the Royal Society of London. Series A, Mathematical and Physical Sciences*, vol. 246, no. 913, pp. 281–294, 1953.

[25] S. Chapman, "The equatorial electrojet as detected from the abnormal electric current distribution above Huancayo, Peru, and elsewhere," *Archives of Meteorological Geophysicae and Bioclimatology*, vol. 4, no. 1, pp. 368–390, 1951.

[26] T. G. Cowling, "The magnetic field of sunspots," *Monthly Notices of the Royal Astronomical Society*, vol. 94, no. 1, pp. 39–48, 1933.

[27] M. Sugiura and J. C. Cain, "A model equatorial electrojet," *Journal of Geophysical Research*, vol. 71, no. 7, pp. 1869–1877, 1966.

[28] J. Lilensten and P.-L. Blelly, *Du SOLEIL à la TERRE : Aéronomie et météorologie de l'espace*, Presses Universitaires de Grenoble, Grenobles, 2000.

[29] J.-P. Legrand and P. A. Simon, "Solar cycle and geomagnetic activity: a review for geophysicists. I-the contributions to geomagnetic activity of shock waves and of the solar wind. II-the solar sources of geomagnetic activity and their links with sunspot cycle activity," *Annales geophysicae*, pp. 565–593, 1989.

[30] J.-L. Zerbo, C. Amory Mazaudier, F. Ouattara, and J. Richardson, "Solar wind and geomagnetism: toward a standard classification of geomagnetic activity from 1868 to 2009," *Annales Geophysicae*, pp. 421–426, 2012.

[31] J.-L. Zerbo, F. Ouattara, C. Amory-Mazaudier, J.-P. Legrand, and J. D. Richardson, "Solar activity, solar wind and geomagnetic signatures," *Atmospheric and Climate Sciences*, vol. 3, no. 4, pp. 610–617, 2013.

[32] W. E. Sawadogo, F. Ouattara, and M. N. Ali, "The effects of the recurrent storms on Fof2 at Ouagadougou Station during solar cycles 21-22," *International Journal of Geosciences*, vol. 10, no. 1, pp. 80–90, 2019.

[33] K. Guibula, *Modélisation par IRI 2012 de la variabilité de fof2 lors des activités géomagnétiques à la station de Korhogo de 1992 à 2002*, Université Norbert ZONGO, Koudougou, 2019.

[34] D. A. Gnabahou, F. Ouattara, E. Nanéma, and F. Zougmoré, "foF2 diurnal variability at African equatorial stations: dip equator secular displacement effect," *International Journal of Geosciences*, vol. 4, no. 8, pp. 1145–1150, 2013.

[35] D. A. Gnabahou, S. A. Sandwidi, and F. Ouattara, "foF2 long-term trend at a station located near the crest of the equatorial ionization anomaly," *International Journal of Geosciences*, vol. 11, no. 8, pp. 518–528, 2020.

[36] J. M. Faynot and P. Vila, "F region at the magnetic equator," *Annales de Geophysique*, vol. 35, pp. 1–9, 1979.

[37] F. Ouattara and C. Amory-Mazaudier, "Solar-geomagnetic activity and Aa indices toward a standard classification," *Journal of Atmospheric and Solar - Terrestrial Physics*, vol. 71, no. 17–18, pp. 1736–1748, 2009.

[38] F. Ouattara, C. Amory-Mazaudier, M. Menvielle, P. Simon, and J.-P. Legrand, "On the long-term change in the geomagnetic activity during the 20th century," in *Annales Geophysicae*, vol. 27, no. 5pp. 2045–2051, Copernicus GmbH, 2009.

[39] J.-L. Zerbo, F. Ouattara, C. Zoundi, and A. M. F. Gyébré, "Solar cycle 23 and geomagnetic activity since 1868," *La Revue CAMES: La Série A*, vol. 12, no. 2, pp. 255–262, 2011.

[40] D. A. Gnabahou and F. Ouattara, "Ionosphere variability from 1957 to 1981 at Djibouti station," *European Journal of Scientific Research*, vol. 73, no. 3, pp. 382–390, 2012.

[41] C. Lal, "Solar wind and equinoctial maxima in geophysical phenomena," *Journal of Atmospheric and Solar - Terrestrial Physics*, vol. 60, no. 10, pp. 1017–1024, 1998.

[42] F. Ouattara and J. L. Zerbo, "Ouagadougou station F2 layer parameters, yearly and seasonal variations during severe geomagnetic storms generated by coronal mass ejections (CMEs) and fluctuating wind streams," *International Journal of Physical Sciences*, vol. 6, no. 20, pp. 4854–4860, 2011.

[43] K. Guibula, F. Ouattara, and D. A. Gnabahou, "foF2 seasonal asymmetry time variation at Korhogo Station from 1992 to 2002," *International Journal of Geosciences*, vol. 9, no. 4, pp. 207–213, 2018.

[44] H. Rishbeth and R. Edwards, "The isobaric _F_ 2-layer," *Journal of Atmospheric and Terrestrial Physics*, vol. 51, no. 4, pp. 321–338, 1989.

[45] H. Rishbeth, I. C. Müller-Wodarg, L. Zou et al., "Annual and semiannual variations in the ionospheric F2-layer: II. Physical discussion," in *Annales Geophysicae*, vol. 18, pp. 945–956, Springer-Verlag, 2000.

[46] I. G. Richardson, E. W. Cliver, and H. V. Cane, "Sources of geomagnetic activity over the solar cycle: relative importance of coronal mass ejections, high-speed streams, and slow solar

wind," *Journal of Geophysical Research, Space Physics*, vol. 105, no. A8, pp. 18203–18213, 2000.

[47] I. G. Richardson, E. W. Cliver, and H. V. Cane, "Sources of geomagnetic storms for solar minimum and maximum conditions during 1972–2000," *Geophysical Research Letters*, vol. 28, no. 13, pp. 2569–2572, 2001.

[48] I. G. Richardson, H. V. Cane, and E. W. Cliver, "Sources of geomagnetic activity during nearly three solar cycles (1972–2000)," *Journal of Geophysical Research: Space Physics*, vol. 107, no. A8, pp. SSH 8-1–SSH 8-13, 2002.

[49] P. Mayaud, "A hundred-year series of geomagnetic data, 1868-1967: indices aa, storm sudden commencements," *IAGA Bulletin*, vol. 33, p. 256, 1973.

[50] J.-L. Zerbo, C. Amory-Mazaudier, and F. Ouattara, "Geomagnetism during solar cycle 23: characteristics," *Journal of Advanced Research*, vol. 4, no. 3, pp. 265–274, 2013.

[51] M. Menvielle, "A possible geophysical meaning of K indices," *Annales de Geophysique*, vol. 35, pp. 189–196, 1979.

[52] J. Meeus, "Astronautique 1960-1961," *Ciel et Terre*, vol. 78, p. 115, 1962.

[53] P.-N. Mayaud, *Derivation, meaning, and use of geomagnetic indices*, vol. 22, American Geophysical Union, Washington, DC, 1980.

[54] D. Vijaya Lekshmi, N. Balan, S. Tulasi Ram, and J. Liu, "Statistics of geomagnetic storms and ionospheric storms at low and mid latitudes in two solar cycles," *Journal of Geophysical Research: Space Physics*, vol. 116, no. A11, 2011.

[55] E. Bramley and M. Peart, "Diffusion and electromagnetic drift in the equatorial _F_ 2-region," *Journal of Atmospheric and Terrestrial Physics*, vol. 27, no. 11–12, pp. 1201–1211, 1965.

[56] B. G. Fejer, "The equatorial ionospheric electric fields. A review," *Journal of Atmospheric and Terrestrial Physics*, vol. 43, no. 5–6, pp. 377–386, 1981.

[57] H. Chandra, H. Sinha, and R. Rastogi, "Equatorial electrojet studies from rocket and ground measurements," *Earth, Planets and Space*, vol. 52, no. 2, pp. 111–120, 2000.

[58] J. M. Forbes, "The equatorial electrojet," *Reviews of Geophysics*, vol. 19, no. 3, pp. 469–504, 1981.

[59] J.-L. Le Mouël, P. Shebalin, and A. Chulliat, "The field of the equatorial electrojet from CHAMP data," in *Annales Geophysicae*, vol. 24, no. 2pp. 515–527, Copernicus GmbH, 2006.

[60] L. F. McNamara, *The Ionosphere: Communications, Surveillance, and Direction Finding*, Krieger Publishing Company, Malabar, FL, 1991.